A FOUR-SWITCH THREE-PHASE INVERTER-FED IM DRIVES AT LOW SPEEDS USING ARTIFICIAL NEURAL NETWORK

[1]**KAVALKAR RAVINDER,** Avanthi institute of engineering and technology.

[2]**DR.M.SURENDER REDDY,** Assistant Professor, Avanthi institute of engineering and technology.

ABSTRACT: This project displays a speed controller utilizing an ANN for circuitous field-arranged control (IFOC) of acceptance engine (IM) drives bolstered by a four-switch three-stage (FSTP) inverter. In the proposed approach, the IM drive system is encouraged by a FSTP inverter rather than the customary six-switch three-stage (SSTP) inverter for practical low-power applications. The proposed ANN enhances dynamic reactions, and it is likewise composed with decreased calculation trouble. The total IFOC conspire fusing the ANN for IM drives nourished by the proposed FSTP inverter is worked in MATLAB/Simulink, and it is additionally tentatively executed continuously utilizing a DSP-DS1103 control board for a model 1.1-kW IM. The dynamic execution, robustness, and lack of care of the proposed ANN with the FSTP inverter-sustained IM drive is analyzed and contrasted with a customary FLC controller under speed following, load unsettling influences, and parameters variety, especially at low speeds. It is discovered that the proposed ANN is more robust than the FLC under load aggravations, and parameters variety. In addition, the proposed FSTP IM drive is equivalent with a conventional SSTP IM drive, thinking about its great dynamic execution, cost decrease, and low aggregate harmonic distortion (THD).

INTRODUCTION

THREE-PHASE induction motors have been considered one of the most commonly used electric machines in industrial applications due to their low cost, simple, and robust construction. Three-phase inverters are considered an essential part in the variable speed ac motor drives. Previously, the traditional six-switch three-phase (SSTP) inverters have been widely used in different industrial applications. These inverters have some drawbacks in low-power range applications, which involve extra cost; the six switches losses, and complicated con trol schemes. Moreover, they require building interface circuits to produce six pulse width modulation (PWM) pulses [1]–[3]. The development of low-cost motor drive systems is an important topic, particularly for a low-power range. Therefore, the three-phase inverter with reduced component for driving an induction motor (IM) was presented in [1]. Also, reduced switch count has been extended for a rectifier–inverter system with active input current shaping [2]. Three different configurations of IM drives fed from a four-switch inverter to implement low cost drive systems for low-power range applications have been presented in [3].

Recently, different research works to design new power converters for minimizing losses and costs have been proposed. Four-switch three-phase (FSTP) inverters instead of SSTP inverters have been used in motor drives [4]–[9], renewable energy applications [10], and active power filters [11], [12]. Control of FSTP brushless dc motor drives has been presented in [4]; using direct torque control (DTC) with non sinusoidal back EMF [5], using single current sensor [6], or using DTC with reduced torque ripples [7]. Compensation of inverter voltage drop in DTC for FSTP PM brushless ac drives has been presented in [8]. A DTC strategy for FSTP-inverters with the emulation of the SSTP inverter operation has been presented in [9]. An FSTP inverter has been presented for renewable energy source integration to a generalized unbalanced grid-connected system [10].

Some features of FSTP inverters over the traditional SSTP inverters have been achieved such as minimized switching losses, decreased cost due to reduction in switches number, reduced number of interface circuits, simpler control schemes to pro duce logic pulses, low computational burden, and more reliability because of lesser interaction between switches [13]–[17]. The PWM method of FSTP inverters has been improved in [13]. However, it requires more voltage sensors. The problem associ ated with FSTP inverter has been further investigated in [14]. A method to produce PWM pulses to control the FSTP-inverters and compensation of capacitor unbalance has been proposed in [15]. A DC–AC FSTP SEPIC-based inverter has been presented in [16]. This inverter improves the utilization of the dc bus compared to the traditional FSTP inverter. Motor current unbalance of FSTP inverters has been studied with a compensation method utilizing current feedback [17].

The control of IMs is a challenging issue as a result of their nonlinear model and parameters variation. In classical control systems using fuzzy logic(FLC) and, the controller performance is significantly reliant on the IM models. However, most of these models are complicated and parameters dependent. Also, they use some assumptions that cause inaccuracy in the mathematical model. Therefore, the model-based controllers, such as a

traditional FLC controllers, cannot give satisfactory performance under speed tracking changes, load impact, and parameters variation [18]. Several works to design the speed controller of electrical motor drives to overcome the problem of fixed gains FLC controllers are recently proposed such as a sliding-mode control with disturbance compensation [19], adaptive pid controller [20], model predictive direct control [21], online inertia identification algorithm for FLC parameters optimization [22], and a data-based FLC controller [23].

In recent years, extensive research works have been presented to implement artificial intelligent controllers (AICs) owing to their merits compared to classic FLC and pid controllers. The major merits of AICs are that they are independent of the plant mathematical model and their performances are robust under system nonlinearities and uncertainties [18], [24]–[29]. AICs techniques for SSTP inverters-fed IM drive systems include fuzzy-logic controller (FLC) [18], [24], self-tuned neuro-fuzzy controller [25]–[27], emotional intelligent controller [28], and adaptive fuzzy sliding-mode control [29]. Also, the FLC for IPMSM-based FSTP inverters has been developed in [30].

The rotor flux is essential for an accurate operation of indirect field-oriented control (IFOC) of IM drives. The field-orientation technique needs precise machine parameters to guarantee accurate decoupling of the stator current vector in relation to the rotor flux vector. Using sensors for direct measurement of the rotor flux gives correct value without sensitivity to machine parameters. Nevertheless, this method is problematic, costly, and prone to errors in noisy environments. Therefore, flux estimation based on the dynamic model of the IM is highly required for high-performance IFOC of IM drives. A problem is that actual machine parameters vary with operating conditions. Inaccurate machine parameters may cause torque non linearity and saturation of the motor. It is possible that the machine control performance degrades due to the parameters mismatch and the system becomes detuned. Consequently, the flux estimation should be as insensitive to varying parameters as possible, which is critical to ensure correct field-orientation control. The flux estimation with its different techniques is a challenge for both speed-sensored and speed-sensorless drives [31]–[36].

In the low-speed region, the effect of changing the motor parameters (stator and rotor resistances as well as the moment of inertia) is considered of utmost importance. For speeds lower than 2/3 maximum motor speed, the performance of FSTP inverters is similar to SSTP inverters because the maximum common-mode voltage from an FSTP is 2/3 of the maximum common-mode voltage from traditional SSTP inverters [3], [15]. Then, the stable operation of FSTP inverters is till 2/3 of the maximum speed. For speeds above 2/3 maximum motor speed, FSTP inverters need extra dc-link voltage to achieve IFOC and develop the same performance of the drive system with SSTP inverters.

Previous works have been reported on the application of the FLC-based IM drive [18], [24]–[29]. Also, few works have been presented for the FLC-based IM fed from the FSTP inverter. However, these works were restricted to high-speed region, and low-speed region is not examined [30]. Thus, it is essential to expand FLC-based IM drives during low and high speeds. Also, these works do not provide any results about the effectiveness of the FLC under parameters uncertainty in the low speed region. Therefore, there is a strong need for successful development and real-time implementation of the FLC-based IM fed from FSTP inverter, which will be appropriate for cost-effective low power practical applications. Hence, the most important contribution of this paper compared with other works is to investigate the dynamic performance of FSTP inverter-fed IM drives using the FLC, particularly at low speeds.

This contribution is achieved throughout the following points:

1) Investigate the dynamic performance of an FLC-based FSTP inverter-fed IM for high-performance industrial applications under speed tracking, load disturbance, and parameters variation, particularly at low speeds;

2) Implement the complete IFOC technique of an IM drive fed by the proposed FSTP inverter in MATLAB/Simulink, and also, in real time by a DSP-DS1103 control board for a prototype 1.1-kW IM;

3) Verify the robustness of the proposed FLC in comparison to the traditional FLC controller using simulation and experimental results at different operating conditions;

4) examine the insensitivity of the two controllers to parameters variation, particularly motor inertia and stator and rotor resistances;

5) compare the performance of the proposed FSTP inverter and the SSTP inverter using total harmonic distortion (THD) of the stator current.

MOTOR DYNAMICS AND CONTROL SCHEME

A. Mathematical model of IM and Control Scheme

The representation of the IM in a d−q axis was used, and the control structure relies on the IFOC. Detailed explanation of the IFOC model was presented in [37] for non-repetition. The control structure of the proposed ANN-based IFOC of the IM fed by the FSTP voltage-source inverter (VSI) is

illustrated in Fig. 1. The speed error between the reference and actual motor speeds and the derivative of speed error are the inputs to the ANN and its output is the reference torque Te∗. The reference currents in d–q axis are transformed into the reference motor currents in a–b–c axis by inverse Park's transformation. The differences between reference motor currents and their actual values are the inputs to hysteresis bands of the current-controlled VSI to generate PWM binary signals, which are utilized to activate the switches of the FSTP inverter. The motor voltages are then produced using the switching states of the FSTP inverter and the dc-link voltage.

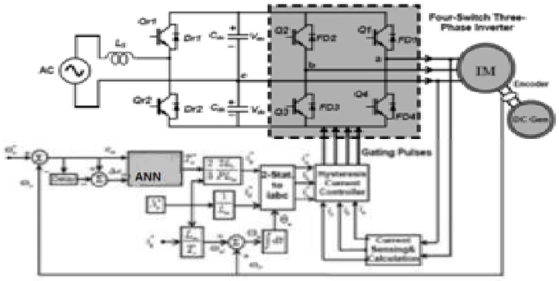

Fig. 1. Block diagram of the proposed ANN-based IFOC scheme of the IM drive fed by FSTP voltage source inverter.

B.FSTP Inverter

Power circuit of an FSTP-VSI-fed IM is illustrated in Fig. 1. This circuit is composed from two sides. The first side is a half-wave voltage doubler fed from a single-phase ac power supply. The frequency of the input ac voltage is fixed; this volt age is rectified using rectifier switches Qr1 and Qr2. The rectifier circuit is utilized to charge the capacitor bank in the dc link. The second side is the FSTP-VSI. The FSTP inverter utilizes four switches: Q1, Q2, Q3, and Q4, respectively, as illustrated in Fig. 1. Phase "a" and phase "b" of the IM are connected through two limbs of the inverter, while phase "c" is connected to the midpoint of the capacitors bank. The FSTP inverter uses four isolated gate bipolar transistors (IGBTs) and four freewheeling diodes to get the two line-to-line voltages Vac and Vcb. However, the third line to line voltage (Vba) is obtained using Kirchhoff's voltage law from a split capacitor bank. The maximum dc-link voltage across each capacitor is equal to Vdc. The generated three-phase output voltages using an FSTP inverter are balanced with adjustable voltage and frequency. In the current analysis, the FSTP inverter switches are considered as ideal switches. The three-phase output voltages of the FSTP inverter are obtained using the dc-link voltages Vdc and the binary signals of the two limbs of the FSTP inverter. The generated phase voltages-fed IM can be expressed as a function of the switching states.

TABLE I
FSTP INVERTER MODES OF OPERATION

Switching Function		Switch ON		Output Voltage Vector		
S_a	S_b			V_a	V_b	V_c
0	0	Q_4	Q_3	$-V_{dc}/3$	$-V_{dc}/3$	$2V_{dc}/3$
0	1	Q_4	Q_2	$-V_{dc}$	V_{dc}	0
1	0	Q_1	Q_3	V_{dc}	$-V_{dc}$	0
1	1	Q_1	Q_2	$V_{dc}/3$	$V_{dc}/3$	$-2V_{dc}/3$

Inverter and V_{dc} as follows [30] :

$$\left.\begin{aligned} V_a &= \frac{V_{dc}}{3}(4S_a - 2S_b - 1) \\ V_b &= \frac{V_{dc}}{3}(-2S_a + 4S_b - 1) \\ V_c &= \frac{V_{dc}}{3}(-2S_a - 2S_b + 2) \end{aligned}\right\} \quad (1)$$

where Vdc is the peak voltage across the storage capacitors; Sa and Sb are the actual states of the two phases "a" and "b" represented by two binary logic variables, which determine the conduction state of the inverter. When Sa is 1, switch (Q1) is conducted and switch (Q4), is not, and when Sa is 0, switch (Q4) is conducted and switch (Q1) is not. Sb has the same principle of operation, and Va, Vb, and Vc are motor phase voltages.

For the balanced generated voltages, the four actual combi nations of the inverter status are lead to four voltage vectors as shown in Fig. 2. Table I illustrates the possible modes of operation and the generated output voltage vector of the FSTP inverter as in [30].

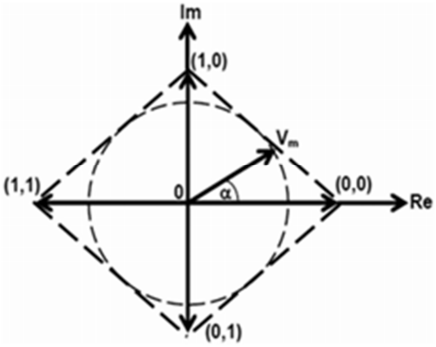

Fig. 2. Switching vectors for an FSTP voltage source inverter

Fig. 3(a) illustrates the simulation study of phase-a current in steady state and its THD at speed 50 r/min under rated load conditions using a FLC controller with an FSTP inverter-fed IM drive. To provide a fair comparison, the simulation study of

steady-state phase-a current and its THD using an FLC with the FSTP-inverter-fed IM drive at similar test conditions are illustrated in Fig. 3(b). It is observed that the motor phase-a current in steady state and its THD of the proposed FLC with the FSTP-inverter-fed IM drive has less THD compared with the traditional FLC controller. Also, the simulation tests of the phase a current in steady state and its THD at speed 50 r/min under rated load conditions using the FLC with an SSTP inverter-fed IM drive is illustrated in Fig. 3(c). It is noted that the FLC using an FSTP inverter-fed IM drive gives less THD compared to the FLC with the traditional SSTP inverter-based method.

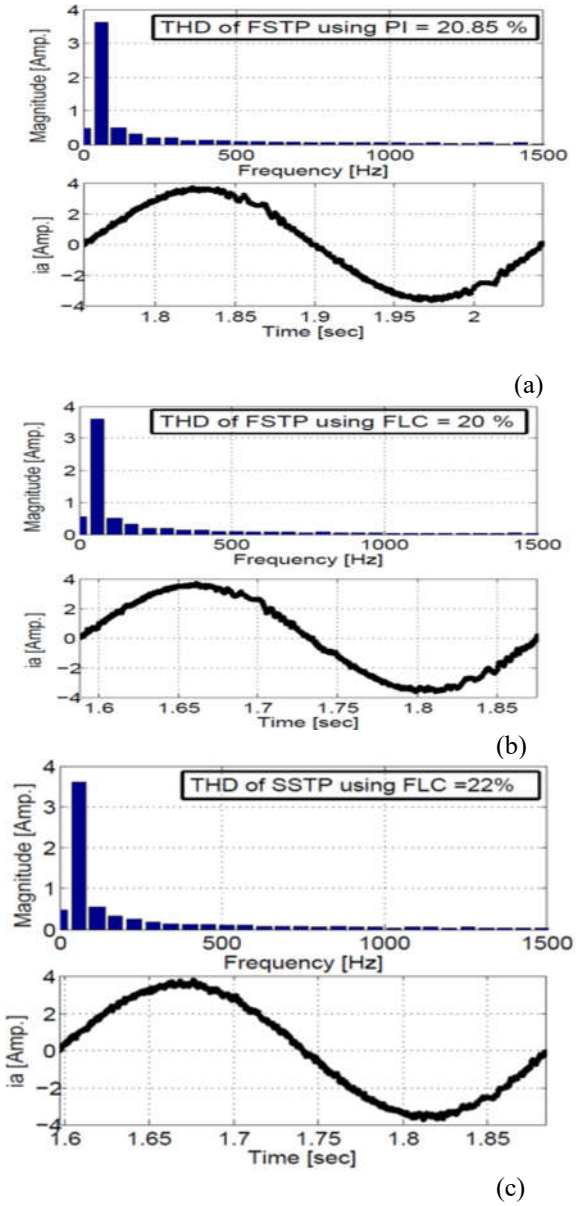

Fig. 3. Simulation results of steady-state phase current ia and its harmonic spectrum at speed 50 r/min under rated load conditions using: (a) FLC controller based FSTP inverter-fed IM drive; (b) FLC-based FSTP inverter-fed IM drive; and (c) FLC-based SSTP inverter-fed IM drive.

SPEED CONTROL METHODS

A.FLC Algorithm

The FLC is used with an IM to overcome the problem of developing accurate mathematical description due to load disturbances and parameters changing. The inputs to the FLC block are the deviation between the reference and actual mo tor speeds (speed error) and speed error derivative. These two inputs are utilized to produce the command torque of an IM (output of the FLC). As illustrated in Fig. 1, the reference torque and reference flux are used to calculate the two reference current components in quadrature and direct axis (i∗ q, i∗ d), respectively. These two currents in combination with the unit vector value are utilized to calculate the three phase reference currents (i∗ a, i∗ b, i∗ c) based on inverse Park's transformation in order to keep the required speed. The main function of the FLC is to keep the motor speed aligned with the desired speed, as a result, the motor currents are kept close to their reference cur rents.

The exact calculations of reference torque depend on the accurate mathematical model of an IM as well as its parameters that are really not constant during the motor operation. The effect of motor parameters variation is only noticeable at low speed of operation, which is considered as a big challenge for accurate calculation of the reference torque, as well as the ex act operation of an IM under the vector control technique. The intelligent controllers, especially an FLC are used with an IM drive to overcome the parameters variation at low-speed operation. The FLC has many features such as, no need for exact mathematical model of an IM, and its action depending on linguistic rules with "IF," "AND," and "THEN" operators. This concept is based on the human logic. The main drawback of the FLC is that it needs high calculation burden for simulation and experimental implementations. Therefore, this paper over comes this problem by designing an FLC with low computation burden. Many membership functions (MFs) shapes can be chosen based on the designer preference and experience. These MFs are characterized by a Gaussian membership. The human perception and experience can be implemented through the MF and fuzzy rules [18]

A. Design of Simplified FLC for IM Drive

The dynamic model of IM expressed as follow

$$T_e = J\frac{d\omega_r}{dt} + B\omega_r + T_L \qquad (2)$$

$$T_e - T_L = J\frac{d\omega_r}{dt} + B\omega_r \quad (3)$$

$$\frac{d\theta_r}{dt} = \omega_r \quad (4)$$

where J is the rotor inertia, Te is the electrical torque, TL is the load torque, B is the frication damping coefficient, and ωr is the motor speed. Employing the small-signal model of an IM, it can be seen that a small change of electrical torque ΔTe results in a small change of the rotor speed Δωr . The electrical motor torque equation rewritten as

$$\Delta T_e = J\frac{d\Delta\omega_r}{dt} + B\Delta\omega_r + \Delta T_L \quad (5)$$

The model of small signal in discrete time for the simplified IM model with applying constant load expressed as

$$\Delta T_e(n) = J\Delta e(n) + B\Delta\omega_r(n) + \Delta T_L \quad (6)$$

This equation describes the developed electrical torque as a function of motor speed error and change of error as follows:

$$T_e(n) = \sum_{n=1}^{N} \Delta T_e(n) = f(\Delta e(n), \Delta\omega_r(n)) \quad (7)$$

where N is the total number of rules. Δωr(n) = ωr∗(n) − ωr(n) is the speed error; Δe(n) = Δωr(n) − Δωr(n − 1) is the change of speed er ror; Δωr(n − 1) is the previous sample of speed error; Δωr(n) is the current value of speed error, ωr(n) is the cur rent value of motor speed, and ωr∗(n) is the present sample of reference motor speed. A MATLAB/Simulink implementation of the FLC is illustrated in Fig. 4. The FLC algorithm of the speed controller employed in the IM drive is based on estimation of two inputs, speed error, and its change as illustrated in Fig. 4. These two linguistic variables are considered as inputs to the system of accordingly interconnected fuzzy-logic (FL) block, and the output is the electrical torque command.

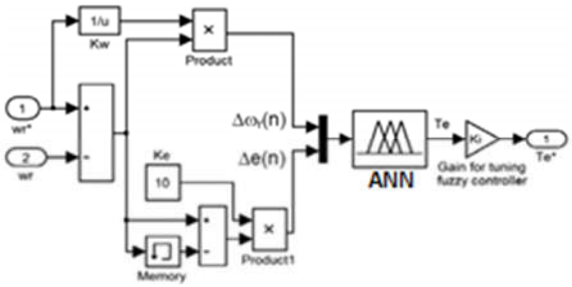

Fig. 4. Block diagram of the ANN using memory block instead of derivative block.

The derivative block can be replaced by time-delay block, which is another way to get the required input. This time-delay block would allow shortening the calculation burden, at the same time also secure the controller from uncertainties in the form of spikes in the out put, which are the drawback of the time-derivative block, if the processed signal change abruptly. The time-delay block would provide a faster and acceptable robust response and as well as precisely accurate tracking of reference speed. It also allows raising the speed sensor sampling rate significantly.

1.Fuzzification Process:

To design the proposed FLC, the first step is to choose the scaling parameters Kw, Ke, and Ki, which are determined for the fuzzification process and receiving the suitable values of the reference torque. The parameters Kw and Ke are determined so that the normalized value of speed error and its change, Δωr(n) and Δe(n), respectively, stays in acceptable limits ±1. The parameter for the output signal Ki is determined so that the rated torque is the output of the FLC at all rated operations. For implementation, the following values are determined Kw = 1/ωr∗ (command speed), Ke = 10, and Ki = 10 in order to obtain the optimal drive simulations and real-time performance. These parameters can be constants or variables and has a significant role for the FLC design in order to obtain a good response during all operating conditions [38]

In this paper, these parameters are considered constants and are selected by experimental trial and error to achieve the best possible drive implementation. The MF's of Δωr(n), Δe(n), and Te(n) are chosen after selecting scaling parameters. MF's are important elements of the FLC. Fig. 5 shows the MFs used for the input and output fuzzy sets of the FLC for producing the reference torque. The triangular MF's are utilized for all the fuzzy sets of the input and output vectors because of their ease of mathematical representation. As a result, they simplify the implementation of the FL inference engine and to reduce the computational burden for real-time operation [40].

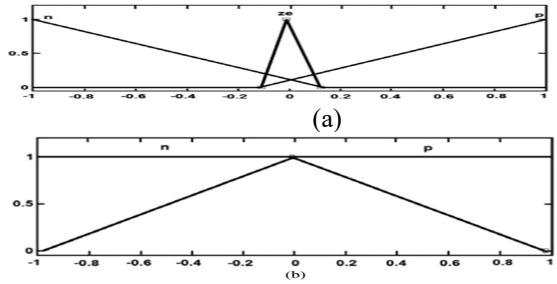

(a)

(b)

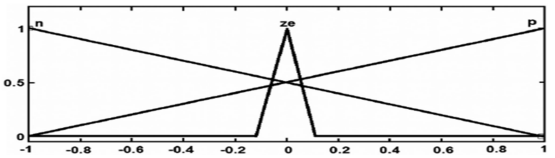

(c)

Fig. 5. Membership functions for: (a) speed error Δωr (n); (b) change of speed error Δe(n); and (c) torque reference Te (n) implemented in MATLAB Simulink.

2. **Rules Base Process:**

The margin of universe of discourse of the input vectors Δωr(n) and Δe(n) and output Te(n) are chosen from –1 to 1. The exact fuzzy rule base of the simplified ANN of the input variables to the output is done by fuzzy IFAND-THEN logic operators rules of six linguistic expressions as described in Table II [39].

TABLE II
RULES BASE PROCESS

1-	IF $\Delta\omega_r(n)$ is N (Negative) AND $\Delta e(n)$ is N (Negative) THEN $T_e(n)$ is ZE (Zero)
2-	IF $\Delta\omega_r(n)$ is ZE (Zero) AND $\Delta e(n)$ is N (Negative) THEN $T_e(n)$ is P (Positive)
3-	IF $\Delta\omega_r(n)$ is P (Positive) AND $\Delta e(n)$ is N (Negative) THEN $T_e(n)$ is P (Positive)
4-	IF $\Delta\omega_r(n)$ is N (Negative) AND $\Delta e(n)$ is P (Positive) THEN $T_e(n)$ is ZE (Zero)
5-	IF $\Delta\omega_r(n)$ is ZE (Zero) AND $\Delta e(n)$ is P (Positive) THEN $T_e(n)$ is ZE (Zero)
6-	IF $\Delta\omega_r(n)$ is P (Positive) AND $\Delta e(n)$ is P (Positive) THEN $T_e(n)$ is P (Positive)

3.Inference and Defuzzification:

Fuzzy inference is the complete process of formulating the mapping of the function from a given input to an output using FL operators. The Mamdani and Sugeno are the two basic types of fuzzy inference methods.

The main difference between these types is the way of defining the output. This paper uses the commonly used method for fuzzy inference and defuzzification process, which is Mam dani max–min (or sum product) composition with the center of gravity method [40]. This method is applied for defuzzification to get Te(n).

Artificial Neural Network

An artificial neural network (ANN), usually called neural network (NN), is a mathematical model or computational model that is inspired by the structure and/or functional aspects of biological neural networks. A neural network consists of an interconnected group of artificial neurons, and it processes information using a connectionist approach to computation. They are powerful tools for modelling, especially when the underlying data relationship is unknown. ANNs can identify and learn correlated patterns between input data sets and corresponding target values. After training, ANNs can be used to predict the outcome of new independent input data. ANNs have been applied to many geotechnical engineering problems such as in pile capacity prediction, modelling soil behaviour, site characterization, earth retaining structures, settlement of structures, slope stability, design of tunnels and underground openings, liquefaction, soil permeability and hydraulic conductivity, soil compaction, soil swelling and classification of soils.

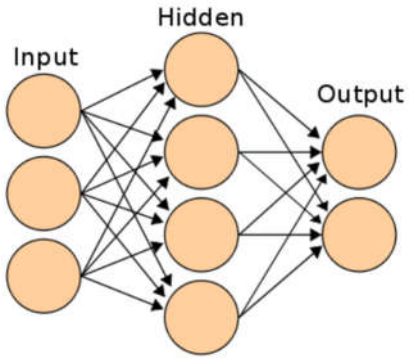

Figure 1: Three layer neural network

Figure1 show three layer neural network consist first layer has input neurons, second layer of hidden neurons, third layer of output neurons. Supervised neural networks are trained in order to produce desired outputs in response to training set of inputs. It is trained by providing it with input and matching output patterns. It used in the modelling and controlling of dynamic systems, classifying noisy data, and predicting future events. Unsupervised neural networks, on the other hand, are trained by letting the network continually adjusting itself to new input.

SIMULATION RESULTS

To validate the effectiveness of the FL speed controller for the FSTP based-IM drive, a simulation model is built by MAT LAB/Simulink. The dynamic performance of the proposed IM drive system has been examined using simulation results under various operating conditions. A fair performance comparison.

A.SPEED TRACKING PERFORMANCE

Fig. 8(a) and (b) demonstrates simulated speed and current signals of the FSTP inverter-fed IM drive using the traditional FLC controller and the proposed ANN scheme, respectively, to see the starting performance. The IM drive starts under light-load torque and a speed command changed from 0 to 100 r/min. As shown in Fig. 8(b), the IM drive using the ANN tracks the desired speed smoothly without any overshoot, undershoot, and steady state error, while the traditional FLC controller has an overshoot and large rising time to arrive the desired speed as shown in Fig. 8(a). However, according to Fig. 8(a) and (b), the stator currents show an overshoot but it lasts for only 0.033 s and its value in the FLC controller is higher than the ANN.

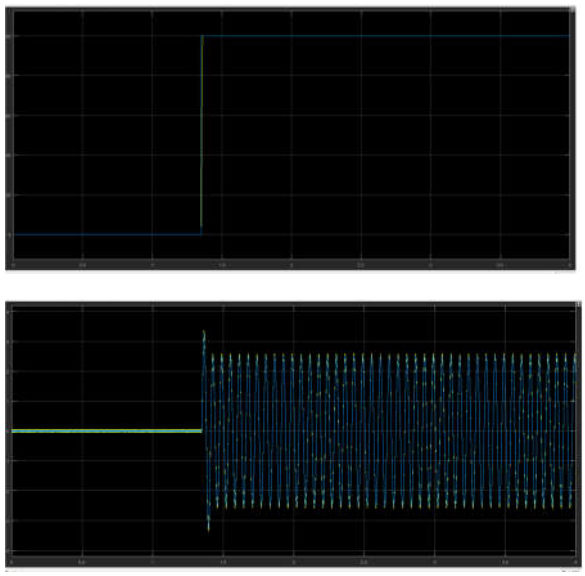

Fig. 8. Simulated speed and stator currents responses of an FSTP inverter fed IM drive for a starting operation at low speed with a step change of a speed reference from 0 to 100 r/min using proposed ANN

Other simulated speed and stator current responses at a sudden speed change are depicted in Figs. 9 and 10 for both the traditional FLC controller and ANN. Also, in these cases, the ANN based IM drive ensures the efficacy over the traditional FLC con troller as the actual speed does not has any overshoot, under shoot, and steady-state error as shown in Figs. 9(b) and 10(b) when compared with the same [see Figs. 9(a) and 10(a)] us ing the traditional FLC controller. Thus, the ANN-based IM drive fed from the FSTP inverter proves a good performance under speed reference tracking.

B.LOAD TORQUE DISTURBANCE

The robustness of an FSTP inverter-fed IM drive for both the traditional FLC controller and ANN is also examined for sudden load change at a speed reference 20 r/min as shown in Fig. 11. At t = 2 s, a rated torque of 7 N·m is applied. It is found that the ANN-based IM drive system confirms the effectiveness over the traditional FLC controller as the actual speed has a low speed dip and recovers quickly with minimum time during sudden load torque, whereas the stator current rapidly arrives to the.new equivalent value of the rated torque. Therefore, good speed tracking performance and good load torque rejection is attained using the ANN-based IM drive, while the FLC-controller-based IM drive is incapable of achieving the desired performance under the sudden change in the reference speed and torque disturbance.

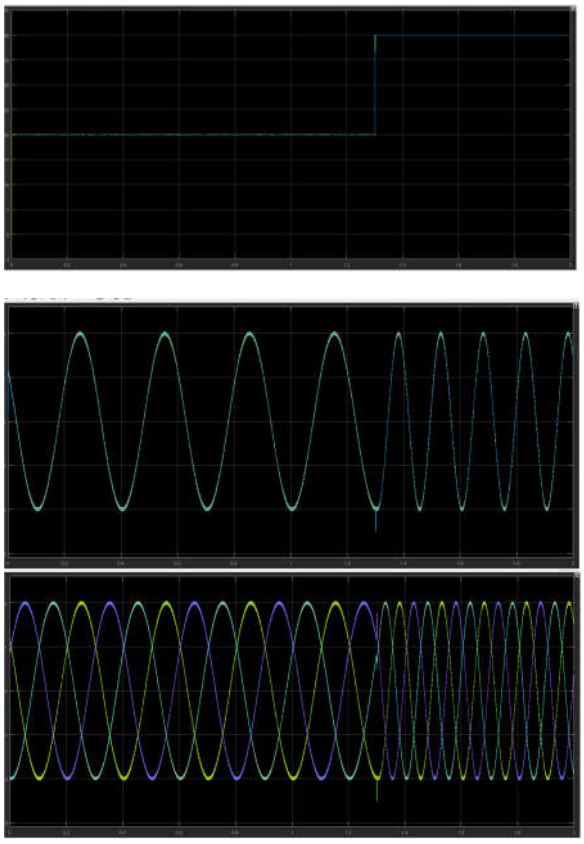

Fig. 9. Simulated speed and stator currents responses of an FSTP inverter-fed IM drive for a step change of a speed reference from 20 to 40 r/min using (a) proposed ANN.

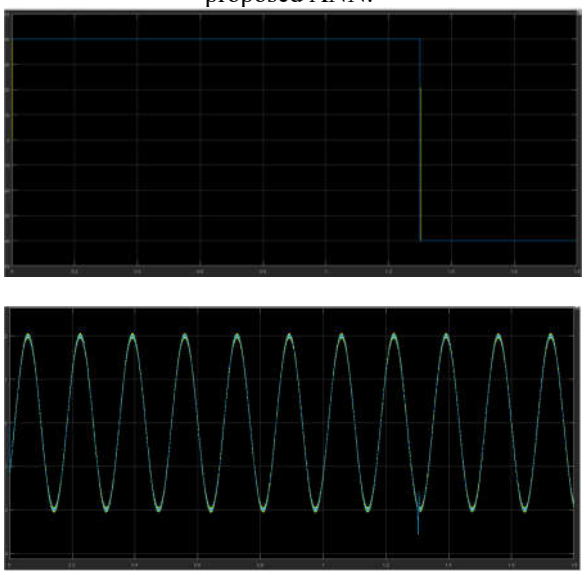

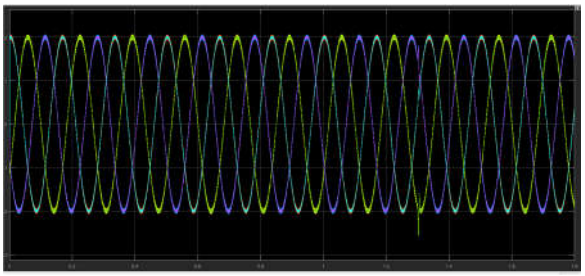

(a)

Fig. 10. Simulated speed and stator currents responses of an FSTP inverter-fed IM drive for a speed reversal from 40 to -40 r/min using (a) proposed ANN.

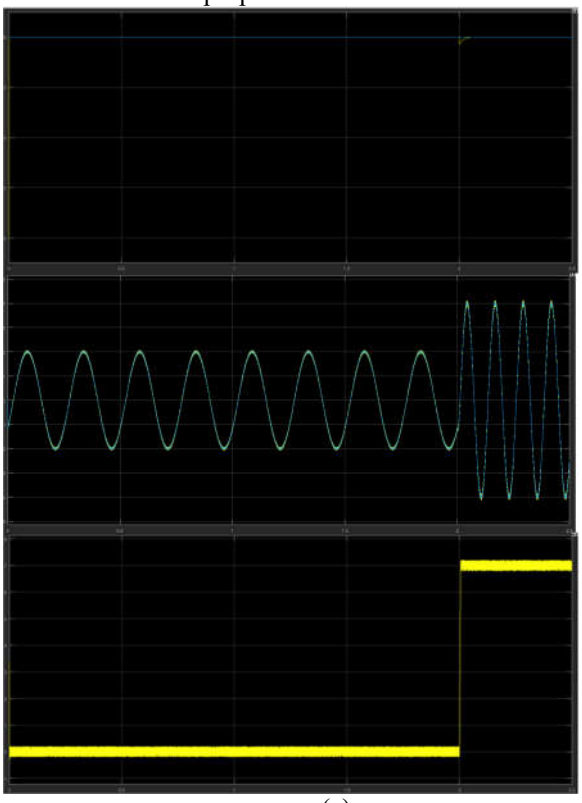

(a)

Fig. 11. Simulated speed and stator currents responses of an FSTP inverter fed IM drive for a sudden increase in load of 7 N·m at a speed reference 20 r/min using (a) proposed ANN.

C.EFFECT OF PARAMETERS VARIATION

The two speed controllers are examined at low speeds under parameters variation. Fig. 12(a) and (b) shows the simulated responses of speed, stator currents, and a quadrature current of an FSTP inverter-fed IM drive for a sudden increase in stator and rotor resistances at a speed reference 20 r/min using the traditional FLC controller and ANN. The mismatch of 100% in the stator and rotor resistance values is tested to prove the robustness of the ANN. The first graph of Fig. 12(b) shows the simulated reference and actual speeds. It is observed that the actual speed tracks the reference speed in spite of stator and rotor resistance mismatches using the proposed ANN. The next graph shows the stator current.

Fig. 12. Simulated speed, stator currents, and quadrature current responses of an FSTP inverter-fed IM drive for a sudden increase in stator and rotor resistances at a speed reference 20 r/min using (a) proposed ANN.

It is clear that the frequency of stator current is changed due to the increase of the slip speed at time t = 1.5 s due to the effect of changing the rotor and stator resistances. The third graph shows the q-component current $i*_q$. It is found that the current $i*_q$ shows insignificant changes at time t = 1.5 s for the mismatches in the rotor and stator resistances. The fourth graph demonstrates the mismatch of 100% in the stator and rotor resistance values that are introduced in the simulation model of the IM at time t = 1.5 s. It is evident in the first graph that the

proposed ANN is robust under parameters mismatch and the speed tracking is not affected. However, the first graph of Fig. 12(a) exhibits a small variation in the speed under the variation of stator and rotor resistances.

Other simulated responses under inertia variation are also presented to examine the robustness of the two speed controllers. The IM drive is tested with inertia (J = 1.5Jo). Fig. 13(a) illustrates simulated speed and trajectory tracking responses of an FSTP inverter-fed IM drive under motor inertia variations for a speed reference of 20 r/min using the traditional FLC controller. The same figure at identical conditions is depicted using the proposed ANN for performance comparison purposes as seen in Fig. 13(b). Fig. 13 justifies the robustness of the proposed ANN in comparison to the traditional FLC controller. As clear, the traditional FLC controller has a substantial variation in the speed response at J = 1.5Jo. However, the proposed FLC remains insensitive under the identical inertia variation. The phase plane trajectory of the second graph in Fig. 13(a) and (b), validates this superiority of the proposed controller.

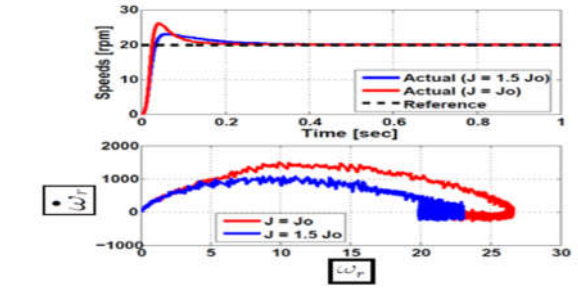

(a)

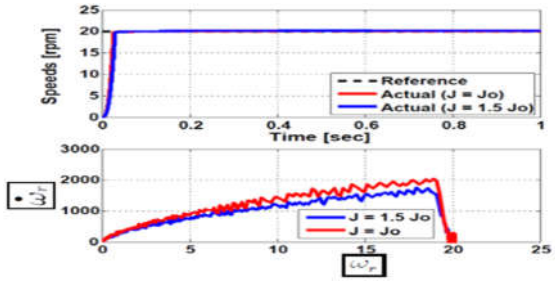

(b)

Fig. 13. Simulated speed and trajectory tracking responses of an FSTP inverter-fed IM drive under motor inertia variations for a speed reference of 20 r/min using (a) traditional FLC controller and (b) proposed FLC.

CONCLUSION

The proposed ANN-based IFOC for an IM drive nourished by a FSTP inverter has been successfully actualized for all intents and purposes by the DSP-DS1103 control board for a research facility 1.1-kW IM and by a PC simulation. The dynamic speed reaction of the IM drive at low speeds is improved utilizing the ANN which is composed with low calculation weight to be proper for constant applications. The legitimacy of the furthered ANN has been inspected in simulation at various speed reference following and load torque unsettling influences, standard low speeds. To affirm the adequacy of the furthered controller, a reasonable execution correlation of the furthered ANN based IM drive with a fuzzy controller has been exhibited. The robustness of the two controllers has been additionally analyzed under parameters variety, particularly engine dormancy, and stator and rotor protections. Relative simulation and exploratory re sults show that the proposed ANN of a FSTP inverter-bolstered IM drive is better than the fuzzy controller under speed following, load aggravations, and parameters variety. The convenience of the ANN has been checked by its high dynamic speed reaction without overshoot and undershoot, and with zero steady-state blunder, and less THD of stator currents. This demonstrates the great capability of the ANN-based IM drive encouraged by a FSTP inverter for practical low-power industrial applications.

TABLE IV
PARAMETERS OF IM

Rated power	1.1 kW	Stator leakage inductance	0.0221 H
Rated current	2.545 A	Mutual inductance	0.4114 H
No. of poles	4	Supply frequency	50 Hz
Stator resistance	7.4826 Ω	Supply voltage	380 V
Rotor resistance	3.6840 Ω	Inertia	0.02 kg·m^2
Rotor leakage inductance	0.0221 H	Rated voltage	380 V

REFERENCES

[1] H. W. van der Broeck and J. D. van Wyk, “A comparative investigation of three-phase inductionmachine drive with a componentminimized voltage fed inverter under different control options,” IEEE Trans. Ind. Appl., vol. IA-20, no. 2, pp. 309–320, Mar./Apr. 1984.

[2] P. Enjeti and A. Rahman, “A new single-phase to three-phase converter with active input current shaping for low cost ac motor drives,” IEEE Trans. Ind. Appl., vol. 29, no. 4, pp. 806–813, Jul./Aug. 1993.

[3] C. B. Jacobina, M. B. R. Correa, E. R. C. da Silva, and A. M. N. Lima, “Induction motor drive system for low power applications,” IEEE Trans. Ind. Appl., vol. 35, no. 1, pp. 52–61, Jan./Feb. 1999.

[4] C.-T. Lin, C.-W. Hung, and C.-W. Liu, “Position sensorless control for four-switch three-phase brushless DC motor drives,” IEEE Trans.

Power Electron., vol. 23, no. 1, pp. 438–444, Jan. 2008.

[5] S. B. Ozturk, W. C. Alexander, and H. A. Toliyat, "Direct torque control of four-switch brushless DC motor with non-sinusoidal back EMF," IEEE Trans. Power Electron., vol. 25, no. 2, pp. 263–271, Feb. 2010.

[6] C. Xia, Z. Li, and T. Shi, "A control strategy for four-switch three-phase brushless DC motor using single current sensor," IEEE Trans. Ind. Elec tron., vol. 56, no. 6, pp. 2058–2066, Jun. 2009.

[7] M. Masmoudi, B. El Badsi, and A. Masmoudi, "DTC of B4-Inverter Fed BLDC motor drives with reduced torque ripple during sector-to sector commutations," IEEE Trans. Power Electron., vol. 29, no. 9, pp. 4855–4865, Sep. 2014.

[8] K. D. Hoang, Z. Q. Zhu, and M. P. Foster, "Influence and compensation of inverter voltage drop in direct torque-controlled four-switch three-phase PM brushless AC drives," IEEE Trans. Power Electron., vol. 26, no. 8, pp. 2343–2357, Aug. 2011.

[9] B. El Badsi, B. Bouzidi, and A. Masmoudi, "DTC scheme for a four switch inverter-fed induction motor emulating the six-switch inverter operation," IEEE Trans. Power Electron., vol. 28, no. 7, pp. 3528–3538, Jul. 2013.

[10] S. Dasgupta, S. N. Mohan, S. K. Sahoo, and S. K. Panda, "Ap plication of four-switch-based three-phase grid-connected inverter to connect renewable energy source to a generalized unbalanced micro grid system," IEEE Trans. Ind. Electron., vol. 60, no. 3, pp. 1204–1215, Mar. 2013.

[11] W. Wang, A. Luo, X. Xu, L. Fang, T. Minh Chau, and Z. Li, "Space vector pulse-width modulation algorithm and DC-side voltage control strategy of three-phase four-switch active power filters," IET Power Electron., vol. 6, no. 1, pp. 125–135, Jan. 2013

[12] X. Tan, Q. Li, H. Wang, L. Cao, and S. Han, "Variable parameter pulse widthmodulation-based current tracking technology applied to four switch three-phase shunt active power filter," IET Power Electron., vol. 6, no. 3, pp. 543–553, Mar. 2013.

[13] F. Blaabjerg, D. O. Neacsu, and J. K. Pedersen, "Adaptive SVM to compensate dc-link voltage ripple for four-switch, three-phase voltage source inverter," IEEE Trans. Power Electron., vol. 14, no. 4, pp. 743–751, Jul. 1999.

[14] R. Wang, J. Zhao, and Y. Liu, "A comprehensive investigation of four switch three-phase voltage source inverter based on double Fourier integral analysis," IEEE Trans. Power Electron., vol. 26, no. 10, pp. 2774–2787, Oct. 2011.

[15] M. B. R. Correa, C. B. Jacobina, E. R. C. Da Silva, and A. M. N. Lima, "A general PWM strategy for four-switch three phase inverters," IEEE Trans. Power Electron., vol. 21, no. 6, pp. 1618–1627, Nov. 2006.

[16] M. S. Diab, A. Elserougi, A. M. Massoud, A. S. Abdel-Khalik, and S. Ahmed, "A four-switch three-phase SEPIC-based inverter," IEEE Trans. Power Electron., vol. 30, no. 9, pp. 4891–4905, Sep. 2015.

[17] J. Kim, J. Hong, and K. Nam, "A current distortion compensation scheme for four-switch inverters," IEEE Trans. Power Electron., vol. 24, no. 4, pp. 1032–1040, Apr. 2009.

[18] M. N. Uddin, T. S. Radwan, and M. A. Rahman, "Performances of fuzzy logic based indirect vector control for induction motor drive," IEEE Trans. Ind. Appl., vol. 38, no. 5, pp. 1219–1225, Sep./Oct. 2002.

[19] X. Zhang, L. Sun, K. Zhao, and L. Sun, "Nonlinear speed control for PMSM system using sliding-mode control and disturbance compensation techniques," IEEE Trans. Power Electronics, vol. 28, no. 3, pp. 1358–1365, Mar. 2013.

[20] J.-W. Jung, V. Q. Leu, T. D. Do, E.-K. Kim, and H. H. Choi, "Adaptive PID speed control design for permanent magnet synchronous motor drives," IEEE Trans. Power Electron., vol. 30, no. 2, pp. 900–908, Feb. 2015.

[21] M. Preindl and S. Bolognani, "Model predictive direct speed control with finite control set of PMSM drive systems," IEEE Trans. Power Electron., vol. 28, no. 2, pp. 1007–1015, Feb. 2013.

[22] L. Niu, D. Xu, M. Yang, X. Gui, and Z. Liu, "On-line inertia identification algorithm for pi parameters optimization in speed loop," IEEE Trans. Power Electron., vol. 30, no. 2, pp. 849–859, Feb. 2015.

[23] M. A. Fnaiech et al., "A measurement based approach for speed control of induction

machines," IEEE J. Emerg. Sel. Topics Power Electron., vol. 2, no. 2, pp. 308–318, Jun. 2014.

[24] M. Masiala, B. Vafakhah, J. Salmon, and A. M. Knight, "Fuzzy self-tuning speed control of an indirect field-oriented control induction motor drive," IEEE Trans. Ind. Appl., vol. 44, no. 6, pp. 1732–1739, Nov./Dec. 2008.

[25] M. Nasir Uddin and Hao Wen, "Development of a self-tuned neuro-fuzzy controller for induction motor drives," IEEE Trans. Ind. Appl., vol. 43, no. 4, pp. 1108–1116, Jul./Aug. 2007.

[26] M. Nasir Uddin, Z. R. Huang, and A. B. M. Siddique Hossain, "Development and implementation of a simplified self-tuned neuro–fuzzy based IM drive," IEEE Trans. Ind. Appl., vol. 50, no. 1, pp. 51–59, Jan./Feb. 2014.

[27] M. Hafeez, M. Nasir Uddin, N. A. Rahim, and H. Wooi Ping, "Self-tuned NFC and adaptive torque hysteresis-based DTC scheme for IM drive," IEEE Trans. Ind. Appl., vol. 50, no. 2, pp. 1410–1419, Mar./Apr. 2014.

[28] G. R. Arab Markadeh, E. Daryabeigi, C. Lucas, and M. Azizur Rahman, "Speed and flux control of induction motors using emo tional intelligent controller," IEEE Trans. Ind. Appl., vol. 47, no. 3, pp. 1126–1135, May/Jun. 2011.

[29] A. Saghafinia, H. Wooi Ping, M. Nasir Uddin, and K. Salloum Gaeid, "Adaptive fuzzy sliding-mode control into chattering-free IM drive," IEEE Trans. Ind. Appl., vol. 51, no. 1, pp. 692–701, Jan./Feb. 2015.

[30] M. Nasir Uddin, T. S. Radwan, and M. Azizur Rahman, "Fuzzy-logic controller-based cost-effective four-switch three-phase inverter-fed IPM synchronous motor drive system," IEEE Trans. Ind. Appl., vol. 42, no. 1, pp. 21–30, Jan./Feb. 2006.

[31] Habib-ur Rehman, "Elimination of the stator resistance sensitivity and voltage sensor requirement problems for DFO control of an induction machine," IEEE Trans. Ind. Electron., vol. 52, no. 1, pp. 263–269, Feb. 2005.

[32] R. Krishnan and F. C. Doran, "Study of parameter sensitivity in high performance inverter-fed induction motor drive systems," IEEE Trans. Ind. Appl., vol. IA-23, no. 4, pp. 623–635, Jul./Aug. 1987.

[33] P. L. Jansen and R. D. Lorenz, "A physically insightful approach to the design and accuracy assessment of flux observers for field oriented induc tion machine drives," IEEE Trans. Ind. Appl., vol. 30, no. 1, pp. 101–110, Jan./Feb. 1994.

[34] G. C. Verghese and S. R. Sanders, "Observers for flux estimation in induction machines," IEEE Trans. Ind. Electron., vol. 35, no. 1, pp. 85–94, Feb. 1988.

[35] H. Kubota, K. Matsuse, and T. Nakano, "DSP-based speed adaptive flux observer of induction motor," IEEE Trans. Ind. Appl., vol. 29, no. 2, pp. 344–348, Mar./Apr. 1993.

[36] M. Hinkkanen and J. Luomi, "Parameter sensitivity of full-order flux observers for induction motors," IEEE Trans. Ind. Appl., vol. 39, no. 4, pp. 1135–1127, Jul./Aug. 2003.

[37] Y. A. Kwon and S. H. Kim, "A new scheme for speed-sensorless control of induction motor," IEEE Trans. Ind. Electron., vol. 51, no. 3, pp. 545–550, Jun. 2004.

[38] M. N. Uddin and R. S. Rebeiro, "Online efficiency optimization of a fuzzy-logic-controller-based IPMSM drive," IEEE Trans. Ind. Appl., vol. 47, no. 2, pp. 1043–1050, Mar./Apr. 2011.

[39] C. B. Butt, M. Ashraful Hoque, and M. Azizur Rahman, "Simplified fuzzy-logic-based MTPA speed control of IPMSM drive," IEEE Trans. Ind. Appl., vol. 40, no. 6, pp. 1529–1535, Nov./Dec. 2004.

[40] J.-S. Yu, S.-H. Kim, B.-K. Lee, C.-Y. Won, and J. Hur "Fuzzy-logic based vector control scheme for permanent-magnet synchronous motors in elevator drive applications," IEEE Trans. Ind. Electron., vol. 54, no. 4, pp. 2190–2200, Aug. 2007.

[41] L. Harnefors, S. E. Saarakkala, and M. Hinkkanen, "Speed control of electrical drives using classical control methods," IEEE Trans. Ind. Appl., vol. 49, no. 2, pp. 889–898, Mar./Apr. 2013.

[42] S. Vukosavic, Digital Control of Electrical Drives. New York, NY, USA: Springer.

[43] M. S. Zaky, "A self-tuning PI controller for the speed control of electrical motor drives," Electr. Power Syst. Res., vol. 119, pp. 293–303, 2015.

Author's Profile:

Dr.M.Surender reddy
Currently working as assistant professor in Avanthi Institute of Engineering & Technology

Mail Id:
msurenderreddy06@gmail.com

Kavalkar Ravinder completed B. Tech from Sree dattha institute of engineering and science and pursuing m.tech from Avanthi institute of engineering and technology.

Mail Id:
ravinderkavalkar@gmail.com